



# The 9th International Electronic Conference on Medicinal Chemistry (ECMC 2023)

01–30 November 2023 | Online

## Synthesis and Characterization of Polystyrene- Based Cationic Hydrogels Enriched with Antibacterial Pyrazoles

Chaired by **Dr. Alfredo Berzal-Herranz**  
and **Prof. Dr. Maria Emília Sousa**



*pharmaceuticals*



**Silvana Alfei \***

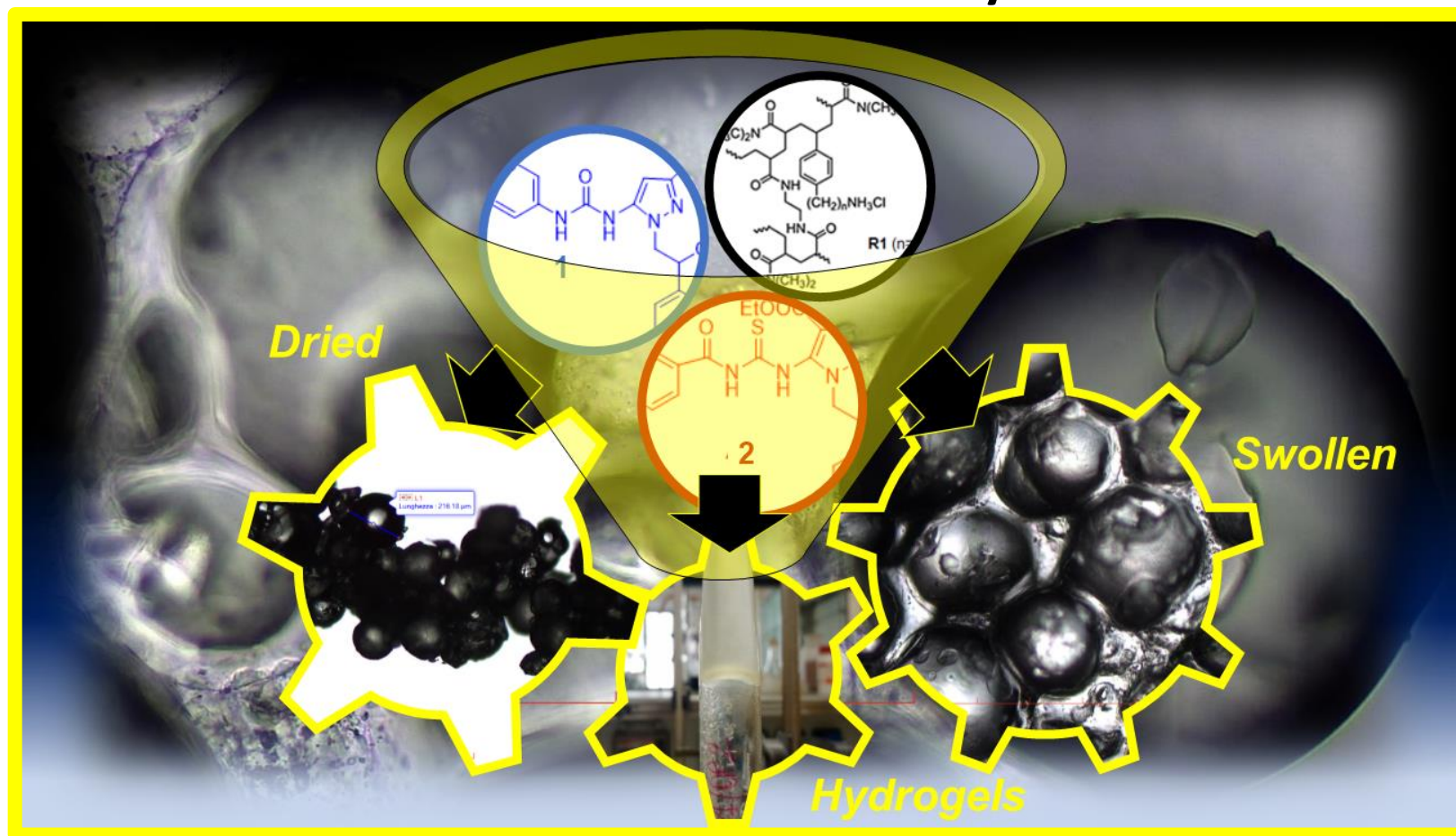
<sup>1</sup> Department of Pharmacy (DIFAR), Section of Chemistry and Pharmaceutical and Food Technologies, University of Genoa, Viale Cembrano, 4, 16148 Genoa, Italy



\* Corresponding author: [alfei@difar.unige.it](mailto:alfei@difar.unige.it)



# Synthesis and Characterization of Polystyrene-Based Cationic Hydrogels Enriched with Antibacterial Pyrazoles





**Abstract:** Recently, we have reported on the antibacterial effects of two pyrazoles (here named 1 and 2) against Gram-positive bacteria. Now, aiming at developing new dermal treatments to cure skin infections sustained by staphylococci, 1 and 2 were formulated as hydrogels, using a synthesized and characterized polystyrene-based cationic resin as gelling agent.

The swelling capability and porosity of the obtained hydrogels were investigated by determining their equilibrium degrees of swelling (EDS) (765% and 675%) and equilibrium water content (EWC) (88% and 87%), which resulted very high, thus establishing for their capability to absorb exudate possibly present on infected skin. Chemometric-assisted ATR-FTIR analyses, as well as optical and scanning electronic microscopy evidenced the chemical structure of gels and their morphology, while the equivalents of  $\text{NH}_3^+$  groups reported to be responsible of antibacterial effects were determined by potentiometric titrations. Weight loss and equilibrium swelling rate, as well as stability studies over times, were also carried out. Rheological experiments were performed to evaluate the flow and dynamic behaviour of the gels, which resulted elastic pseudoplastic fluids, with good spreadability. Collectively, the obtained results support the pyrazole-base hydrogels reported here as new topical treatments to cure severe skin and wound infections sustained by MDR bacteria of *Staphylococcus* genus.

**Keywords:** antibacterial pyrazoles; cationic resin (R1); microsized composite hydrogels; high swelling capability; high porosity, pseudoplastic rheological behavior



## Introduction

Pyrazole derivatives have been widely reported to possess several biological activities, including interesting antimicrobial effects. Pyrazole-based compounds, clinically approved to be used in the treatment of certain pathologies, have subsequently demonstrated significant antimicrobial activity. In this context, we have recently synthesized two tri-substituted pyrazoles containing two phenyl rings and one fluorine atom (**1** and **2**, Figure 1) endowed with promising antibacterial effects, especially against multi drug resistant (MDR) clinical isolates of Gram-positive species (MICs = 32–64  $\mu\text{g}/\text{mL}$ ).

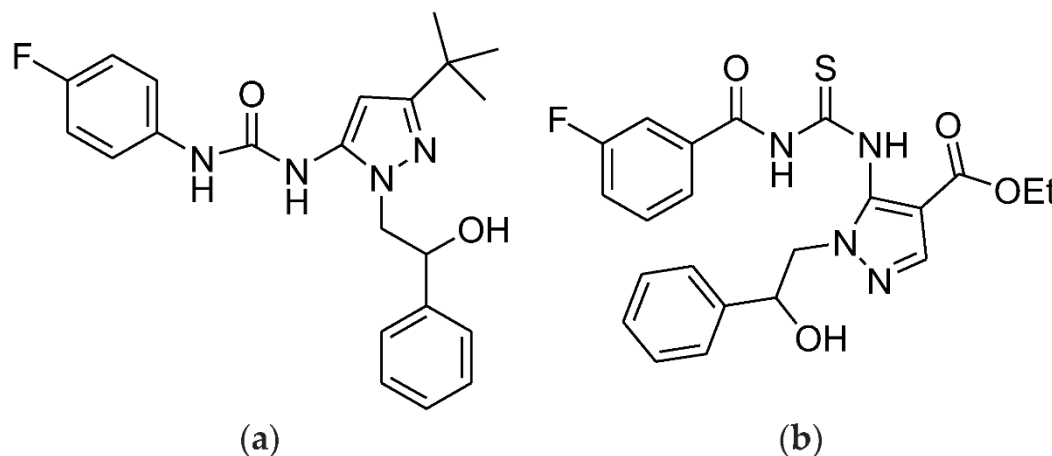
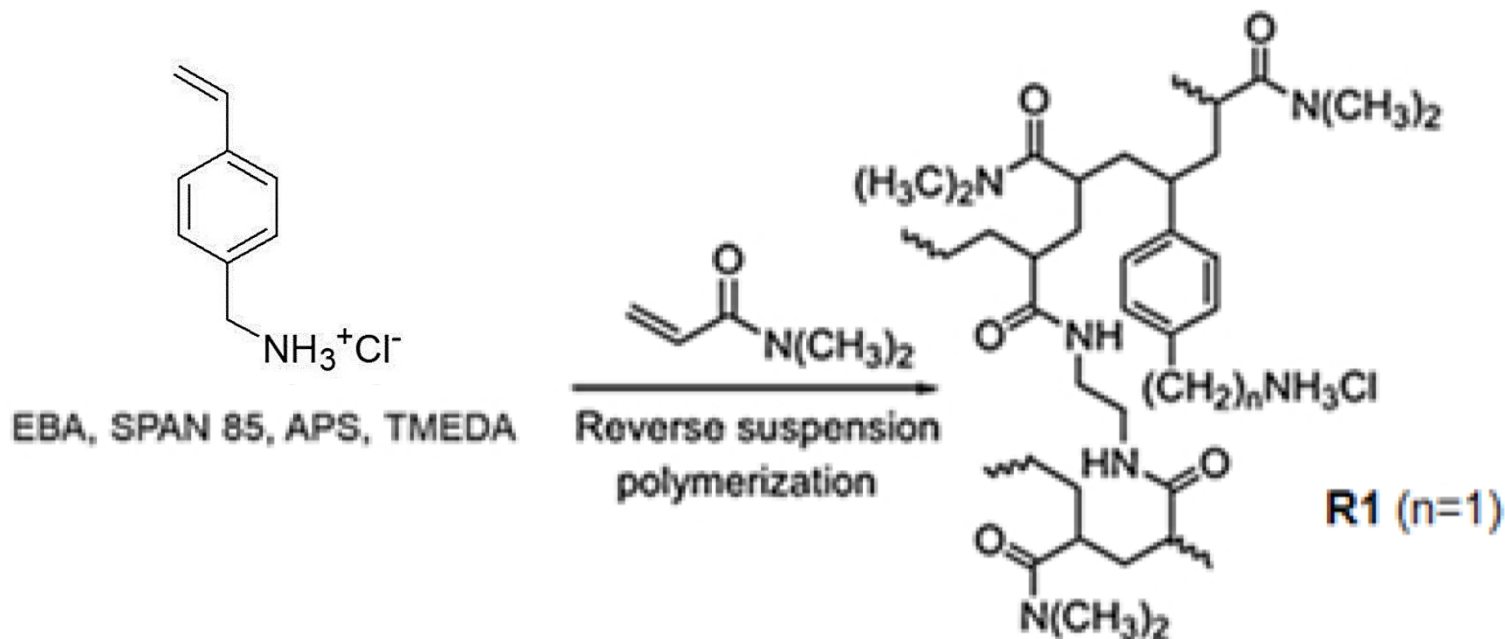


**Figure 1.** Structure of the antibacterial pyrazoles **1** (a) and **2** (b).





Here, aiming at exploiting the antibacterial properties of **1** and **2** and at preparing new dermal treatments to cure skin infections, we used them to obtain pyrazoles-based hydrogels. The polystyrene-based resin (R1) prepared copolymerizing the cationic polystyrene monomer (M1) with DMAA as described in the following Scheme, was used as gelling agent.



EBA = ethyl-bis acrylamide; APS = ammonium persulphate; TMEDA = trimethyl-ethylene diamine



## Results and discussion

### Antibacterial Properties of 1 and 2

On the right, we have reported the MIC values (MICs) ( $\mu\text{g/mL}$ ) of pyrazoles **1** and **2** against Gram-positive bacteria. MICs were obtained from experiments carried out at least in triplicate.

Accordingly, **1** demonstrated activity against vancomycin resistant (VRE) *E. faecium* and *E. faecalis*, methicillin resistant *S. aureus* (MRSA), and *S. epidermidis* (MRSE), while **2** exhibited antibacterial effects specifically against staphylococci.

\* Vancomycin resistant; \*\* methicillin resistant; \*\*\* resistant toward both methicillin and linezolid. Promising antibacterial activity was evinced in bold.

Strains	MICs ( $\mu\text{g/mL}$ )	
	<b>1</b>	<b>2</b>
<i>E. faecalis</i> 450 *	<b>64</b>	>128
<i>E. faecalis</i> 451 *	<b>64</b>	>128
<i>E. faecium</i> 182 *	<b>64</b>	>128
<i>E. faecium</i> 300 *	<b>64</b>	>128
<i>E. faecium</i> 364 *	<b>64</b>	>128
<i>E. durans</i> 103	<b>64</b>	>128
<i>S. aureus</i> 18 **	<b>64</b>	<b>64</b>
<i>S. aureus</i> 187 **	<b>32</b>	<b>64</b>
<i>S. aureus</i> 195 **	<b>32</b>	128
<i>S. epidermidis</i> 180 ***	<b>32</b>	<b>64</b>
<i>S. epidermidis</i> 181 ***	<b>64</b>	<b>64</b>
<i>S. epidermidis</i> 363 **	<b>32</b>	128
<i>S. saprophyticus</i> 41	<b>64</b>	>128
<i>S. warneri</i> 74	<b>64</b>	>128
<i>S. hominis</i> 125 *	<b>64</b>	128
<i>S. lugdunensis</i> 129	<b>32</b>	<b>32</b>

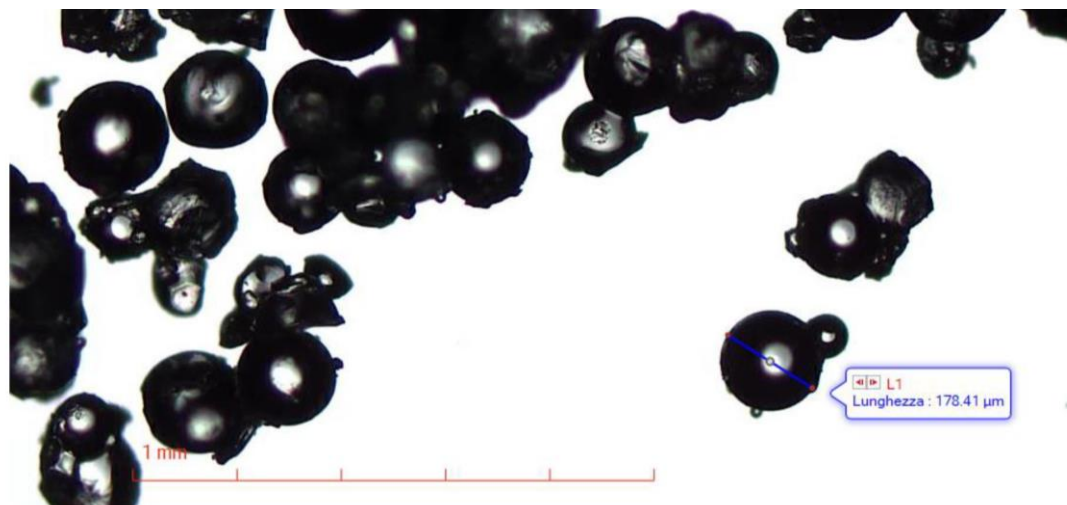


## Antibacterial Properties of 1 and 2 with Reference Antibiotics

Strains	MIC ( $\mu\text{g/mL}$ )				
	<b>1</b>	<b>2</b>	Ampicillin	Ciprofloxacin	Oxacillin
<i>E. faecalis</i> 365 *	128	>128	128	-	-
<i>E. faecalis</i> 450 *	<b>64</b>	>128	128	-	-
<i>E. faecalis</i> 451 *	<b>64</b>	>128	128	-	-
<i>E. faecium</i> 182 *	<b>64</b>	>128	128	-	-
<i>E. faecium</i> 300 *	<b>64</b>	>128	128	-	-
<i>E. faecium</i> 364 *	<b>64</b>	>128	128	-	-
<i>S. aureus</i> 18 **	<b>64</b>	<b>64</b>	-	128	512
<i>S. aureus</i> 187 **	<b>32</b>	<b>64</b>	-	128	512
<i>S. aureus</i> 195 **	<b>32</b>	128	-	128	512
<i>S. epidermidis</i> 180 ***	<b>32</b>	<b>64</b>	-	<b>64</b>	256
<i>S. epidermidis</i> 181 ***	<b>64</b>	<b>64</b>	-	<b>64</b>	256
<i>S. epidermidis</i> 363 **	<b>32</b>	<b>64</b>	-	<b>64</b>	256

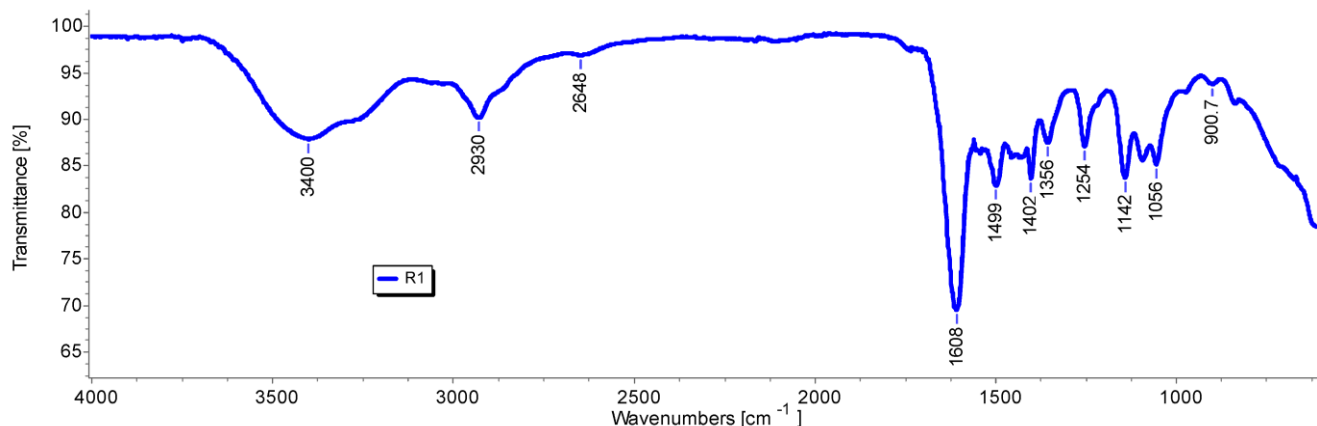


## Optical Microscopy of R1 Particles



R1 particles demonstrated spherical morphology and microsized dimensions in the range 125–250  $\mu\text{m}$ . The  $\text{NH}_2$  equivalents per gram of R1 were determined by the method of Gaur and Gupta and resulted to be  $10.22 \pm 0.059$  mmol/g. The ATR-FTIR spectrum of R1, confirming the presence of both M1 and DMAA is reported below.

## ATR-FTIR spectrum of R1







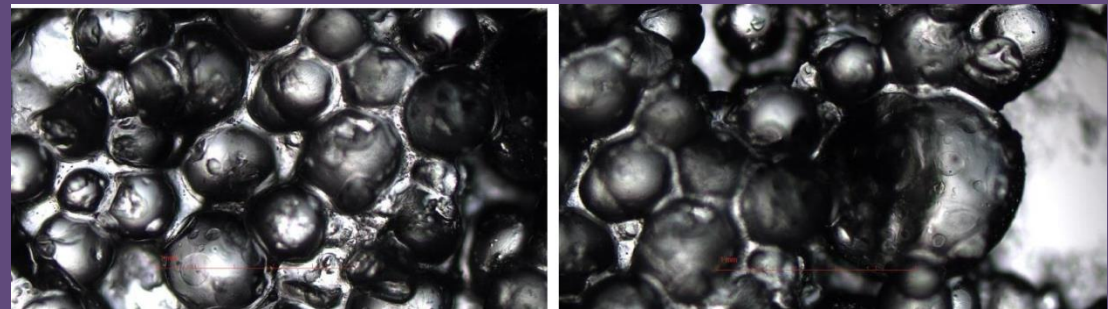
## Preparation of R1HG-1 and R1HG-2 Hydrogels

Data concerning the preparation of pyrazole-enriched hydrogels R1HG-1 and R1HG-2.

Pyr	Vi (mL)	Wi (mg)	R1 Vi/Wi (mL/mg)	R1+Pyr Vi/Wi (mL/mg)	Vf gel (mL)	H <sub>2</sub> O (mL)	Concentration (mg */mL) (%wt */v)	EDS (%)	EWC (%)
<b>1</b>	0.2	21.0	0.45/380.3	0.65/401.3	5.62	4.97	80.7 (8.1) <sup>1</sup>	764.6 <sup>1</sup>	88.4 <sup>1</sup>
<b>2</b>	0.1	33.1	1.00/599.1	1.10/632.2	7.75	6.65	95.1 (9.5) <sup>2</sup>	675.0 <sup>2</sup>	87.1 <sup>2</sup>

Pyr = pyrazole; EDS = equilibrium degree of swelling; EWC = equilibrium water content; Vi = initial volumes of the compounds; Wi = initial weights of the compounds; Vf = volumes of the hydrogels; \* weight of R1+pyrazole; <sup>1</sup> refers to R1HG-1; <sup>2</sup> refers to R1HG-2.

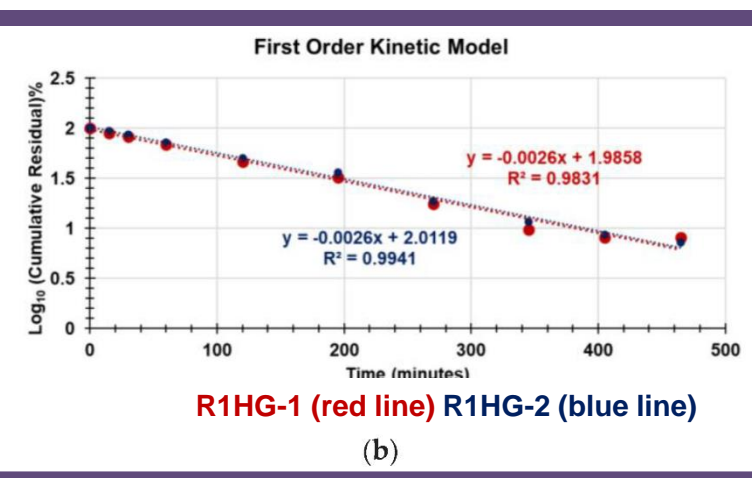
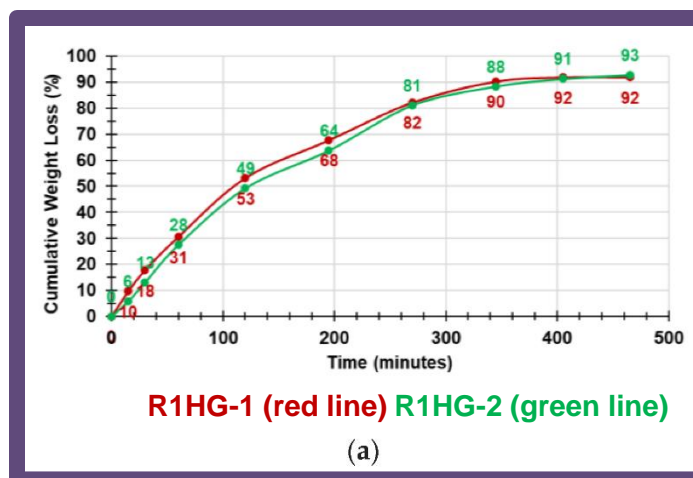
R1HG-1 and R1HG-2 were prepared at their maximum EDS by mixing pyrazoles and R1 in a centrifuge tube, adding an excess of water, stirring, degassing and sonicating. The not adsorbed water was separated by centrifugation and removed.



Spherical particles of swollen hydrogels as appear at optical microscopy.

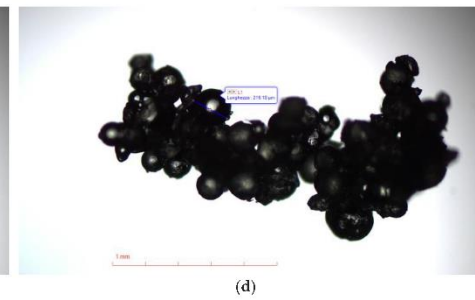
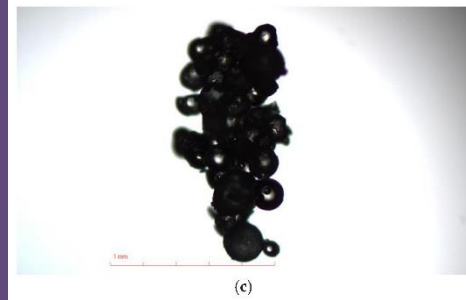
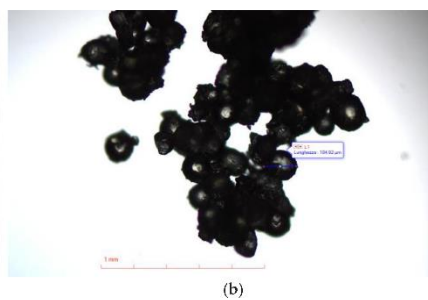
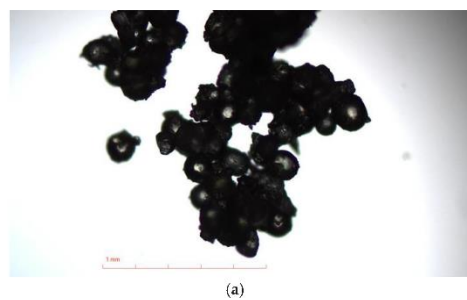


## R1HG-1 and R1HG-2 Hydrogels Characterization: Water Loss



Appearance of R1HG-1 (left)  
and of R1HG-2 (right)

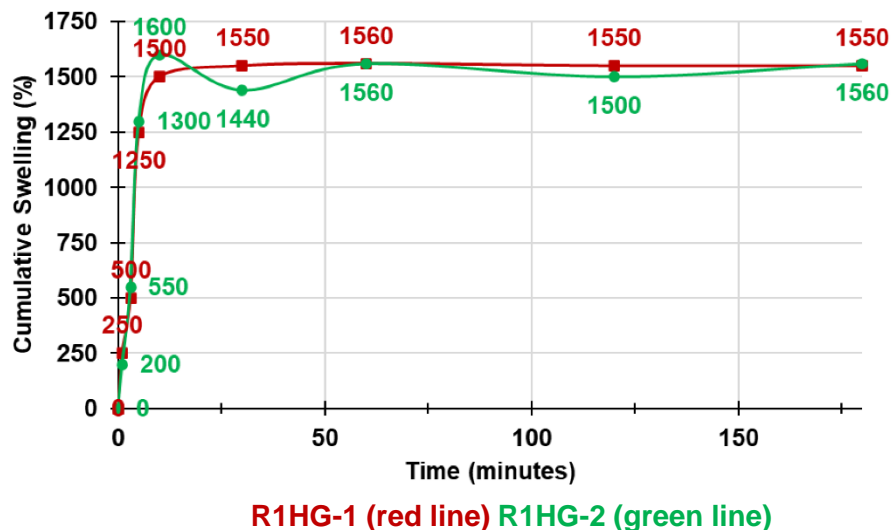
Water loss experiments over time under heating revealed a quantitative release of water for both gels (a) governed by first order kinetics (b), while particles of fully dried gels were like those observed for R1 (below).



Optical micrographs of dried R1HG-1 (a,b) and of R1HG-2 (c,d).

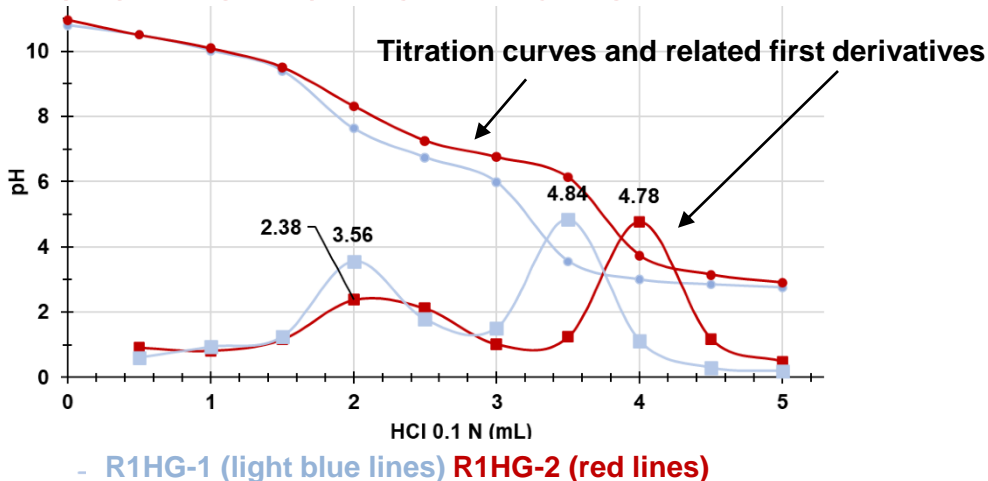


## Equilibrium Swelling Rate



The equilibrium swelling rate ( $Q_{\text{equil}}$ ), was reached after only 10 min by R1HG-2 (1600) and after 60 min by R1HG-1 (1560). Collectively, the equilibrium swelling rates of the two gels were comparable with each other and were like those already reported in literature.

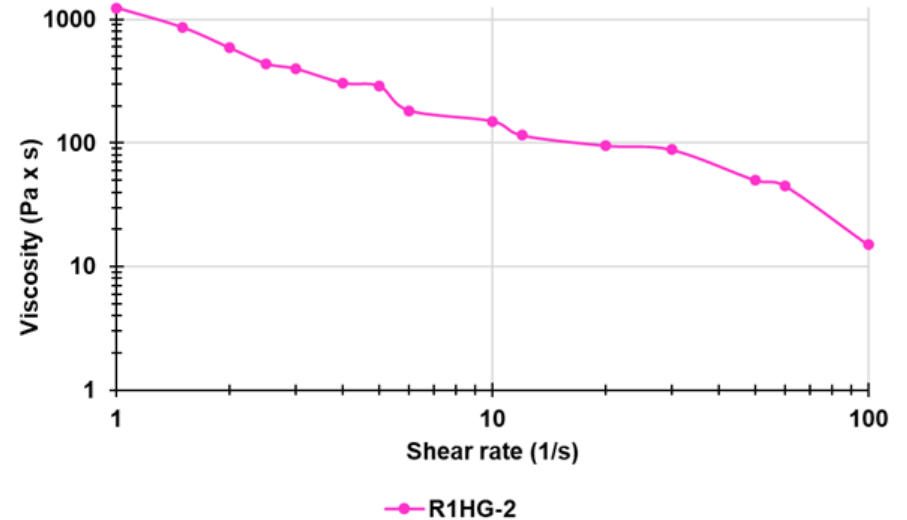
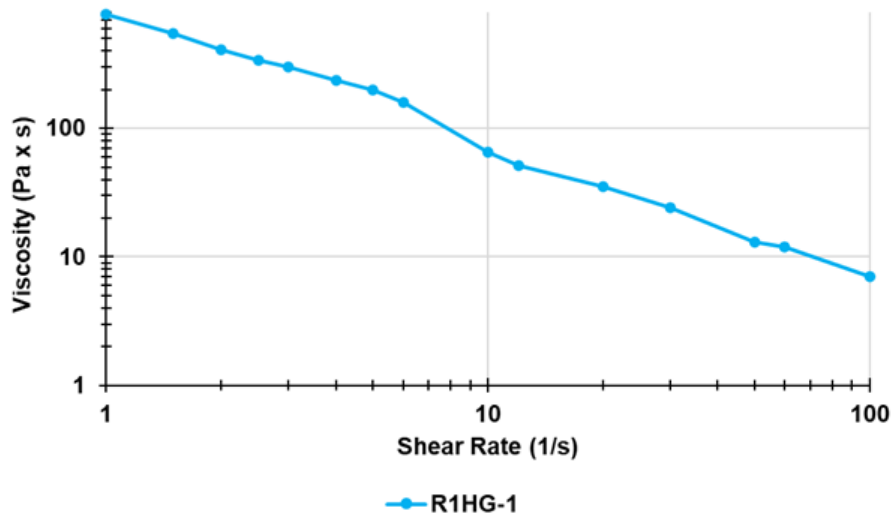
## Potentiometric Titration



The buffer capacity of both pyrazole-based hydrogels was high up to 1.5 mL of HCl 0.1 N added. According to the maxima of the first derivatives, both hydrogels evidenced two end points. The first ones corresponded to the titration of the excess of NaOH added, while the second ones (4.0 mL HCl for R1HG-2 (max 4.78) and 3.5 mL HCl for R1HG-1 (max 4.84) to the titration of the  $\text{NH}_2$  groups. From these data we determined the  $\text{NH}_2$  contents per gram of gel (0.728 mmol/g (R1HG-1) and 0.826 mmol/g (R1HG-2)).



## Rheological Studies

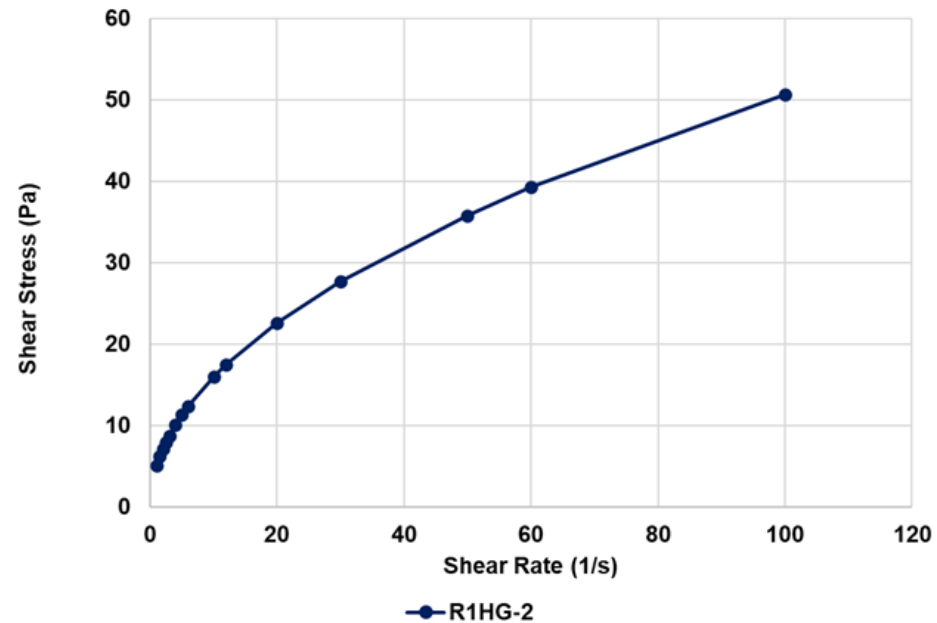
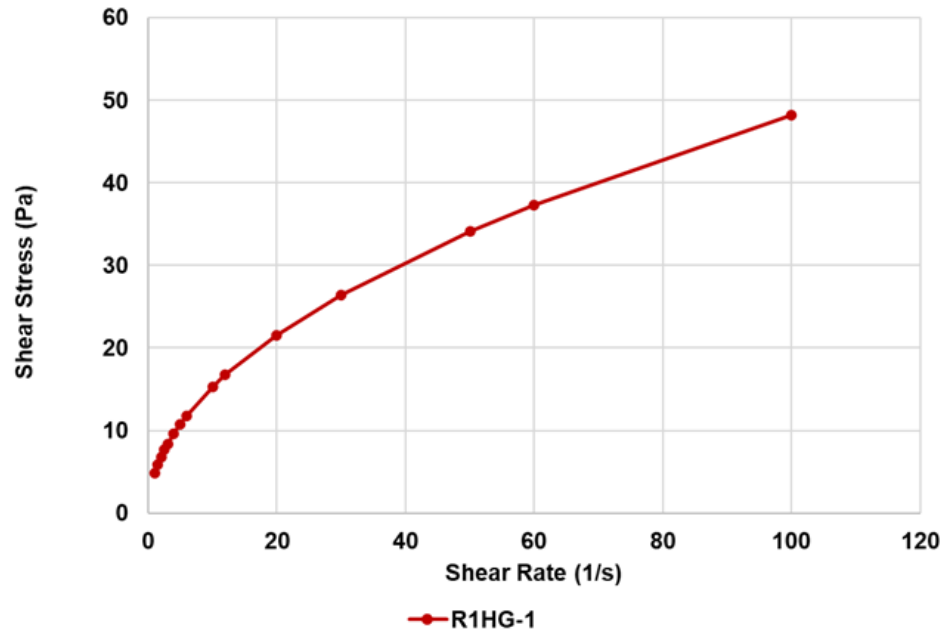


The viscosity curves of **R1HG-1** (left plot) and **R1HG-2** (right plot) were obtained measuring their viscosity as a function of a shear rate applied and the results have been presented in logarithmic scale. Both viscosity profiles evidenced a decreasing of viscosity for increasing of shear rate, thus establishing that our hydrogels are non-Newtonian fluids with a shear thinning behaviour.

Using two different forms of the Cross equation and a reported hybrid mathematical method we determined the shear stress values as a function of shear rate. The related plots are available in the next slide.



## Rheological Studies



The graphs show the plots of the shear stress ( $\tau$ , Pa) vs. shear rate ( $\dot{\gamma}$ ,  $\text{s}^{-1}$ ) of **R1HG-1** (left) and **R1HG-2** (right). According to the plots profiles, both gels were pseudoplastic fluids not having constant  $\eta$  for shear rate values  $< 30$ . Over these values, their  $\eta$  values were constant and they assumed a plastic Bingham behaviour (irreversible deformations). To have confirmation of the shear-thinning behaviour of **R1HG-1** and **R1HG-2** we modelled the data of shear stress vs. shear rate using the Herschel–Bulkley rheological model.



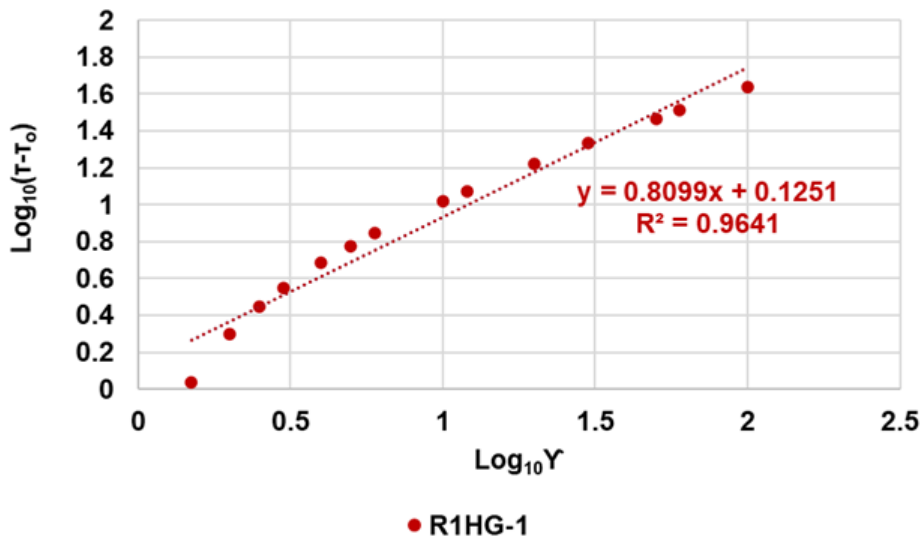


## Rheological Studies

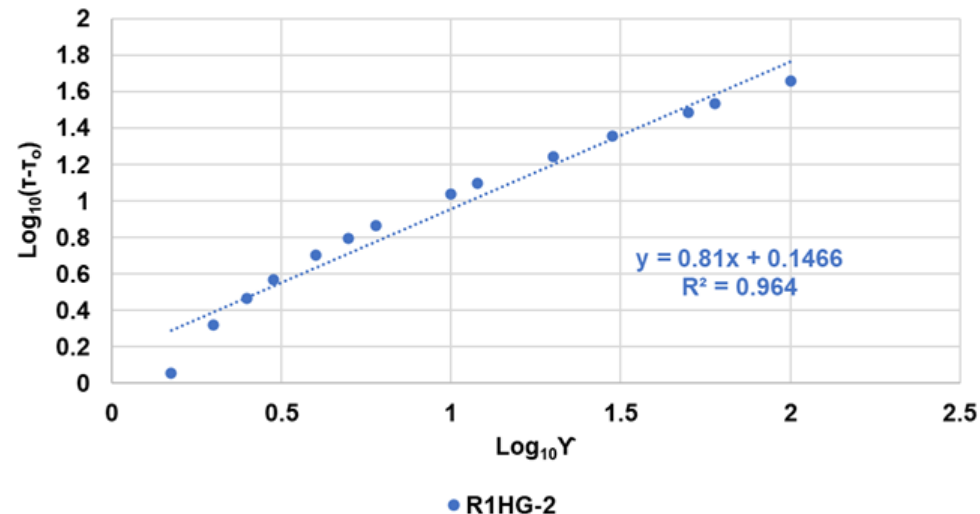
Herschel–Bulkley rheological model is expressed by the equation:  $\tau = \tau_0 H + \kappa H \gamma^n H$  where  $nH$  is the fluid flow behavior index, which indicates the tendency of a fluid to shear thin or thick,  $\kappa H$  is the consistency coefficient, which serves as the viscosity indexes of the systems, and  $\tau_0 H$  is the Herschel–Bulkley yield stress point. When  $\gamma = 0$ ,  $\tau = \tau_0$ .

Following, the Herschel–Bulkley rheograms obtained by reporting in graph  $\text{Log}(\tau - \tau_0)$  vs.  $\text{Log}(\gamma)$  are shown.

Herschel–Bulkley rheogram



Herschel–Bulkley rheogram





## Rheological Studies

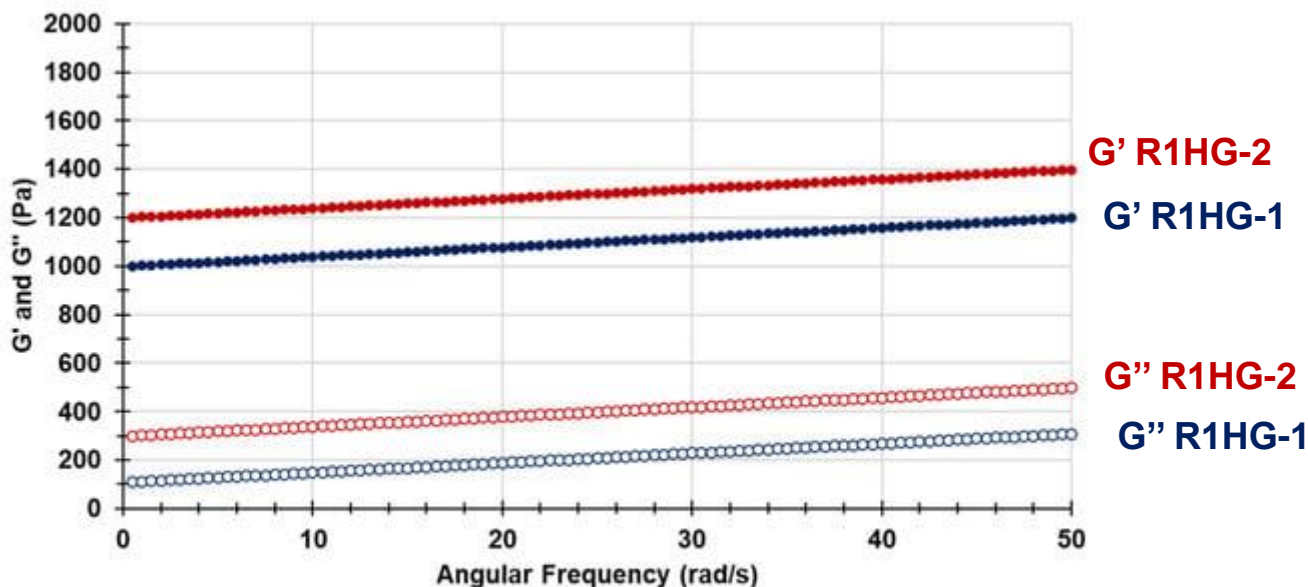
In the plots,  $\text{Log } k$  (corresponding to  $\tau_0$ ) and  $n$  were obtainable from the related linear regression equations, where  $\text{Log } k$  is the intercept and  $n$  is the slope. The  $k$  values were calculated accordingly.

Sample	Equation	$n$	$\text{Log}_{10}K$	$K$	$R^2$
R1HG-1	$Y=0.8099+0.1251$	0.8099	0.1251	-0.9027	0.9641
R1HG-2	$Y=0.81+0.1466$	0.8100	0.1466	-0.8338	0.9640

In both cases  $0 < n < 1$  thus confirming a shear-thinning behaviour and the values of  $\tau_0$  (yield stress) were very low, thus assuring that consistency of both gels could allow for easy spreading on the skin by applying a light massage, in a future topical administration.



## Frequency-Sweep Experiments



Frequency sweep experiments were performed to assess the viscoelastic characteristics of the network structure of R1HG-1 and R1HG-2 and to define the frequency dependence of the  $G'$  and  $G''$  moduli. Experiments were carried out at 1% strain (below the critical strain point of R1HG-1 and R1HG-2) and  $G'$  and  $G''$  values for R1HG-1 and for R1HG-2 were measured in the frequency range ( $\omega$ ) of 0.5–50 Hz. In such conditions, the values of  $G'$  were always higher than those of  $G''$  for both gels and almost independent on the angular frequency, thus establishing that the networks of both gels have an elastic behaviour.



## Conclusions

**1**

**We have synthesized styrene-based cationic microspheres (R1) capable to provide hydrogels upon dispersion in water, by low-cost reverse suspension copolymerization**

**2**

**R1 was characterized and used as gelling agent to formulate two antibacterial pyrazoles (1 and 2) as hydrogels (R1HG-1 and R1HG-2)**

**3**

**Both hydrogels were characterized by PCA-assisted ATR-FTIR analyses, optic microscopy, weight loss experiments, equilibrium swelling rate studies, rheological experiments, while their structural stability was assessed over time at r.t.**



## Conclusions

**1**

**Rheological studies established that R1HG-1 and R1HG-2 are both non-Newtonian Bingham pseudo-plastic fluids with low yield stress**

**2**

**Frequency-sweep experiments established that both hydrogels have an elastic behavior**

**3**

**Collectively, R1HG-1 and R1-HG-2 are promising as topical formulations to treat severe skin infections sustained by MDR Staphylococci**





# The 9th International Electronic Conference on Medicinal Chemistry

01-30 November 2023 | Online



**Thank  
you !**



**Silvana Alfei \***